3003

REPRINT

Ha Bui-Van, Valentin Hamaide, Christophe Craeye, François Glineur and Eloy de Lera Acedo

Direct deterministic nulling techniques for large random arrays including mutual coupling

IEEE Transactions on Antennas and Propagation, 66(11), 5869-5978, 2018

CORE CENTER FOR OPERATIONS RESEARCH AND ECONOMETRICS

CORE
Voie du Roman Pays 34, L1.03.01
B-1348 Louvain-la-Neuve
Tel (32 10) 47 43 04
Email: immaq-library@uclouvain.be
https://uclouvain.be/en/research-institutes/
lidam/core/reprints..html

Direct Deterministic Nulling Techniques for Large Random Arrays Including Mutual Coupling

Ha Bui-Van, Valentin Hamaide, Christophe Craeye, *Senior Member, IEEE*,
François Glineur, and Eloy de Lera Acedo

***Abstract*— Effective approaches for interference nulling in large random planar arrays are presented. Starting from the well-known subtraction technique, it is shown that the suppression is only effective when the mutual coupling is taken into account. Moreover, for practical antennas with significant cross-polarization levels, additional efforts are required to null interference in both co- and cross-patterns. Alternative techniques are proposed to efficiently generate null patterns that are able to suppress interferers from the output of the beamformer of large arrays. In particular, a technique exploiting the polarization diversity of modern multiantenna systems is proposed to effectively suppress a large number of interferers while offering high sensitivity. Examples related to SKA1-LOW stations are presented to illustrate the performance of these techniques. Throughout these examples, the embedded element patterns obtained using fast full-wave simulation techniques are exploited to fully account for the effects of mutual coupling.**

***Index Terms*— Antenna arrays, mutual coupling, radio-frequency interference (RFI) nulling, square kilometer arrays (SKAs).**

I. Introduction

MODERN communication, imaging, and sensing systems are designed with large antenna arrays, offering better capacity, higher resolution, and improved sensitivity. Examples include future massive MIMO systems [1], weather radar [2], as well as the next generation of radio telescopes [3], [4]. Those systems increasingly rely on analog or digital beamforming. The coexistence of these systems, however, presents an issue to be solved, which is radio-frequency interference (RFI). The interference, however, is not limited to man-made radio signal, and it also includes natural interfering sources (e.g., the sun and the brightest stars) for the radio astronomy systems. The interference can be known in prior and/or be time-varying; their cancellation is hence subjected to two different procedures, namely, deterministic and adaptive interference nulling, respectively. There is a strong interest in deterministic nulling, in case the interference directions are known, but not the strength of the signal. The suppression of such interferers is important for applications such as radio astronomy [3], [4], which will be the main focus of this paper. As for adaptive nulling, methods, such as the minimum variance approach, are often implemented [5], but they will not be discussed here. For wideband beamforming, the digital approach offers a lot of flexibility through slicing the bandwidth into many narrow bands.

For known interferers, a beamforming approach [6] can be exploited to generate a null pattern in the direction of the RFI, thus filtering out interference from the output signal. The weights of the beamforming network can be derived either directly, i.e., in a noniterative way or via optimization methods. The direct approaches often start from the definition of the interference subspace [7]–[9]; the weights are then computed by projecting the signal onto the subspace orthogonal to the interferer. These techniques quickly offer solutions for pattern nulling, while the protection of the main beam can be simultaneously considered, e.g., by using a windowed version of the steering vector, as discussed in [8]. On the other hand, the optimization approach considers the nulling goals as a synthesis problem, where the weights are optimized to suppress sidelobes in the directions of interferers, i.e., enforcing the sidelobe to be smaller than a given threshold within a given sector. The optimization approach often allows one to satisfy other constraints, such as minimizing, at the same time the sidelobe level to fully exploit the degrees of freedom offered by the weights. Adaptive interference nulling [10], global optimizations [11], [12], and convex optimization [13] have been used to effectively suppress the sidelobes. The optimization approaches, however, are essentially iterative, which is time-consuming. On large aperture arrays of hundreds and up to thousands of antennas such as LOFAR [3] or square kilometer array (SKA) [4], this required computational time rapidly becomes unaffordable. From this point of view, a direct approach is more suitable.

However, all above-listed works (related to the direct methods) have considered antennas as point sources or assumed antennas to have identical radiation patterns. The solutions, therefore, do not take into account the different element

Manuscript received December 9, 2017; revised May 9, 2018; accepted August 3, 2018. Date of publication September 17, 2018; date of current version October 29, 2018. This work was supported in part by the Science & Technology Facilities Council, U.K., (SKA) under Grant ST/M001393/1 and in part by the University of Cambridge, U.K. *(Corresponding author: Ha Bui-Van.)*

H. Bui-Van is with AGC Inc., Tokyo 100-8405, Japan. He was with ICTEAM, Université catholique de Louvain, 1348 Louvain-la-Neuve, Belgium (e-mail: buivanhabk@gmail.com).

V. Hamaide is with Deloitte Belgium, 1930 Zaventem, Belgium (e-mail: valentinhamaide@yahoo.fr).

C. Craeye and F. Glineur are with ICTEAM, Université catholique de Louvain, 1348 Louvain-la-Neuve, Belgium (e-mail: buivanha@uclouvain.be; valentinhamaide@yahoo.fr; christophe.craeye@uclouvain.be; francois.glineur@uclouvain.be).

E. de Lera Acedo is with the Cavendish Laboratory, Astrophysics Group, University of Cambridge, Cambridge CB3 0HE, U.K. (e-mail: eloy@mrao.cam.ac.uk).

Manuscript received month date, 2017.

Color versions of one or more of the figures in this paper are available online at http://ieeexplore.ieee.org.

Digital Object Identifier 10.1109/TAP.2018.2869068

0018-926X © 2018 IEEE. Personal use is permitted, but republication/redistribution requires IEEE permission.
See http://www.ieee.org/publications_standards/publications/rights/index.html for more information.

patterns that result from mutual coupling. It has been shown in [14] and [15] that this simplification leads to quite shallow nulls, such that interferers are not sufficiently rejected. The inclusion of mutual coupling in the analysis can be carried out via the exploitation of the embedded element patterns (EEPs), which corresponds to the patterns of each element in the presence of all other, passively terminated, antennas. The EEPs are increasingly exploited in antenna array optimization schemes [16]–[19]. Thus, in order to produce deep nulls in the directions of the RFIs using existing techniques, the EEPs need to be incorporated. Moreover, the polarization of interferers can be random even for known sources. It is difficult to track the polarization of interferers and to align the antennas. Since practical antennas have significant cross-polarization levels, the nulling algorithm thus needs to suppress interference in both polarizations at the same time. This paper presents a family of new direct techniques to suppress RFI in both copolarization and cross-polarization patterns while including the effects of mutual coupling. A general approach is first derived by forming two sets of orthogonally polarized beams in the directions of interferers and applying the subtraction technique to obtain null patterns. A pseudoinverse solution is then taken, which ensures a minimum variation among magnitudes of excitations. The technique is applicable to a wide range of arrays made of single-port or multipolarized antennas. For modern systems [2]–[4] designed with antennas having dual or diverse polarizations, an extension is proposed exploiting the polarization diversity of the array. The extra degrees of freedom from other polarizations allow one to effectively generate zero radiation in the RFI directions while offering high sensitivity. Finally, a simple and yet effective approach based on the simultaneous construction of the main beam and nulls is presented. Again, a solution based on the pseudoinverse approach is obtained for excitation vectors. It is worth noting that all of these techniques are direct, as the weighting vectors are obtained through a simple noniterative procedure.

The remainder of this paper is organized as follows. In Section II, the deterministic nulling approach is explained. The subtraction technique, algebraically equivalent to the orthogonal projection approach, is first presented. Then, the mutual coupling effect is included by exploiting the information contained in the EEPs. Solutions for single- and dual-polarization pattern nulling are then proposed. In Section III, numerical examples are shown for the case of the Square Kilometer Array Low-frequency station (SKA1-LOW) [20] using the proposed techniques. Several examples, including pure single-polarization, linear, and dual-polarization arrays made of SKA log-periodic antennas (SKALAs) [20], are used to test the proposed techniques. Finally, an extreme case, where a large number of nulls are created to reject fields from a whole domain, is discussed. Conclusions and perspectives are drawn in Section IV.

II. Deterministic Nulling With Mutual Coupling

Three direct approaches for deterministic interference nulling are detailed in this section. To better understand the proposed techniques, the subtraction, or orthogonal projection approach [8], is first recalled. The solutions to include mutual coupling are then proposed for single- and dual-polarized arrays. The following presentation concerns a single-beam pattern. The method can be applied straightforwardly to multibeam arrays. Moreover, the discussion is considering interferers located outside the main beam. When interference is within the main beam, other techniques are more suitable, such as the model-based cancellation [21].

A. Subtraction Technique: Scalar Case

Denoting by y the column vector of received voltages at antenna ports, the output of the beamformer is obtained as

$$b = y^T w \tag{1}$$

where w is the column vector of beamformer weights and ^{T} denotes the transpose operation. To filter out the interference signal from the output of beamformer, one needs to select w, such that the pattern of the array consists of nulls in the directions of RFIs [8]. In the following, the derivation of w is presented based on the subtraction technique while including mutual coupling.

Let us consider a 2-D array of N elements, in which element n, located at Cartesian coordinates (x_n, y_n), is characterized by an EEP $\vec{f}_n(\theta,\phi)$, whose reference center is at the position of the element n. θ is the angle between the radiation direction and the zenith. ϕ is the azimuth angle starting from the X-axis. The radiation direction is defined as $(u, v, w) = (\sin\theta\cos\phi, \sin\theta\sin\phi, \cos\theta)$. The array pattern, scanned in direction (θ_0, ϕ_0) via an excitation vector w_0, is expressed as

$$\vec{F}(\theta,\phi) = \sum_{n=1}^{N} \vec{f}_n(\theta,\phi)\ w_{0,n}\ \mathrm{e}^{-jk(ux_n+vy_n)}. \tag{2}$$

In the following, a simple representation of the array pattern will be obtained based on matrix-vector products. To this end, the embedded patterns are first phased-shifted, such that the reference for the phase corresponds to the center of the array. Second, the two polarization components are represented by two scalar quantities. This defines two matrices E^p and E^q with as many rows as (θ,ϕ) directions and as many columns as antennas, with

$$E^p(m,n) = \vec{f}_n(\theta_m,\phi_m)\cdot \hat{a}_p\ \mathrm{e}^{-jk(ux_n+vy_n)} \tag{3}$$

an entry (m, n) of E^p from the antenna n and direction (θ_m, ϕ_m), where $\hat{a}_p$ is a unit vector representing polarization p in direction (θ_m, ϕ_m). The E^q matrix is defined similarly for the other polarization. From there, (2) can be rewritten as

$$\vec{F}(\theta,\phi) = E^p w_0 \hat{a}_p + E^q w_0 \hat{a}_q. \tag{4}$$

In this paper, p and q denote the copolarization and cross polarization, respectively, which could also be vertical/horizontal or TE/TM polarization patterns, depending on which of the three Ludwig's definitions [22] is used.

We start with the scalar field case and then proceed to the vector case in Section II-B. By scalar, we mean considering only one polarization component of the pattern, e.g., copolarization pattern, E^p. The case of arrays with identical elements,

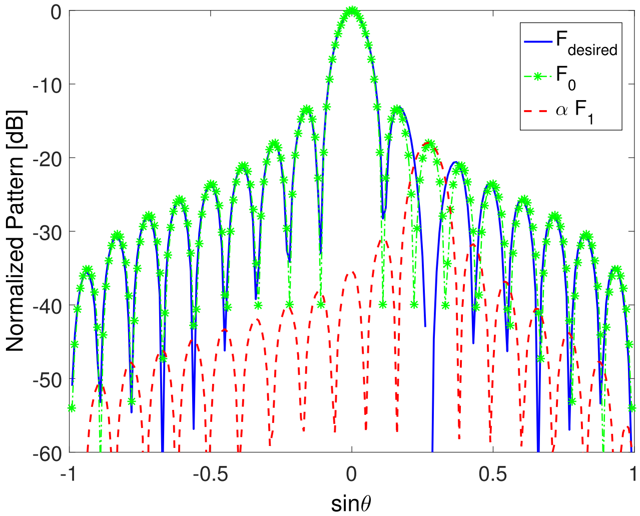

Fig. 1. Subtraction approach: the null pattern (F_{desired}) is a result of the subtraction of the original pattern, F_0, obtained by w_0 and the pattern steered at null direction F_1 using w^i.

which neglects mutual coupling, can be cast in the scalar case, since the isolated pattern is assumed identical for all elements and can be factored out of (2). Thus, in that case, we need only the matrix E^p to store the phase for each element.

For M known interferer directions, the subtraction technique [8] is carried out by: 1) generating beams in the direction of the interference and 2) subtracting a scaled version of the interferer beams from the original pattern, as shown in Fig. 1. The nulls are created by imposing

$$E(\Omega^{rfi})(w_0 - w^{rfi}\alpha) = 0 \tag{5}$$

where $E(\Omega^{rfi})$ are the rows of E corresponding to the directions of all interferers $\Omega^{rfi} = (\theta^{rfi}, \phi^{rfi})$, and thus, $E(\Omega^{rfi})$ has size $M \times N$, w^{rfi} is an $N \times M$ matrix with each column containing coefficients for steering the beam in a given interferer direction, and α is the $M \times 1$ vector of scaling coefficient multiplying the patterns in the interferers' direction.

For the scalar case, E consists of E^p only, and the vector α is then derived as

$$\alpha = (E^p(\Omega^{rfi})w^{rfi})^{-1}E^p(\Omega^{rfi})w_0. \tag{6}$$

The resulting weighting vector for the array is then expressed as

$$w = w_0 - w^{rfi}\alpha = (I - w^{rfi}(E^p(\Omega^{rfi})w^{rfi})^{-1}E^p(\Omega^{rfi}))w_0 \tag{7}$$

where I is the identity matrix. If $M = N$, i.e., the number of RFIs directions is equal to the number of antennas, a trivial solution of (7) is $w = 0$. This scenario is, however, avoided to ensure the quality of the nulls [8] and $M \ll N$, i.e., the number of RFIs is always smaller than the total number of antennas. Equation (7) can be identified in [8, eq. (2)] for the case of isotropic radiators or when EEPs are considered identical, by equating $w^{rfi} = V$ and $V^H = E^p(\Omega^{rfi})$, since in this case, $E^p(\Omega^{rfi})$ is a matrix containing the phase factors needed to steer the array in the RFIs directions, which is V^H in [8]. More generally, (7) accounts for all the effects of mutual coupling by using EEPs (here for the copolarization).

B. Subtraction Technique With Full Pattern: Vector Case

Practical antennas often have both copolarization and cross-polarization patterns, where the cross-polar pattern can be significantly high with respect to the copolar pattern level in the sidelobe region. To properly suppress the RFI signals, one needs to generate nulls in both patterns. In other words, twice as many conditions need to be satisfied, which leads to the construction of two beams in each RFI direction, with significantly different polarizations. These beams are characterized by weight matrices w_1 and w_2 of size $N \times M$ (one column per RFI direction), respectively, multiplied by scaling vector α_1 and α_2. Equation (5) written for both polarization patterns, i.e., vector case, is then

$$\begin{bmatrix} E^p(\Omega^{rfi}) \\ E^q(\Omega^{rfi}) \end{bmatrix} \left(w_0 - \begin{bmatrix} cccw_1 & w_2 \end{bmatrix} \begin{bmatrix} \alpha_1 \\ \alpha_2 \end{bmatrix} \right) = \begin{bmatrix} 0 \\ 0 \end{bmatrix} \tag{8}$$

or

$$\begin{bmatrix} E^p(\Omega^{rfi})w_0 \\ E^q(\Omega^{rfi})w_0 \end{bmatrix} = \begin{bmatrix} ccccE^p(\Omega^{rfi})w_1 & E^p(\Omega^{rfi})w_2 \\ E^q(\Omega^{rfi})w_1 & E^q(\Omega^{rfi})w_2 \end{bmatrix} \begin{bmatrix} \alpha_1 \\ \alpha_2 \end{bmatrix}. \tag{9}$$

In this case, $2M$ beams are created to suppress M interferers in each pattern. To ensure the quality of nulls, the two following conditions need to be satisfied: 1) $2M \ll N$ and 2) the beams created using w_1 and w_2 are sufficiently independent. The former condition is generally satisfied as modern antenna arrays often consist of hundreds to thousands of elements as in the SKA case. The second requirement ensures that (8) is not ill-conditioned and there are always exact solutions for α_1 and α_2.

For arrays made of antennas with a single excitation port, i.e., providing single linear/circular polarization, a subarray approach can be applied to (9), where two subarrays are selected forming $2M$ beams in the M RFIs directions. In particular, for each RFI direction, following the subtraction methodology, two beams (weights w_1 and w_2) with sufficiently different polarizations are created. Those two beams are created using two different subarrays (although those subarrays could be overlapping, i.e., be partially composed of common elements). Equation (9) can then be solved directly. The optimal selection of subarrays (e.g., based on their sensitivity) is an open subject, which is not addressed in this paper. A discussion on this approach is presented in Section IV, while a general solution will be given later.

For modern communication and sensing systems, the arrays are often made of dual-/multiple-polarized antennas to improve the performance [2], [4], i.e., each polarization is controlled by a separate beamforming network or an independent excitation. Using these antennas, the subarray approach is no longer necessary. Equivalently, each subarray is made of all radiators associated with a given excitation. Indeed, for dual-polarized arrays, one can easily generate two sets of independent beams steering at RFIs for (9) by setting w_1 that is equal to $\exp(-jk(u_i x_n + v_i y_n))$ for the first excitation (i.e., exciting the first polarization) and 0 for the second excitation and w_2 that is equal to $\exp(-jk(u_i x_n + v_i y_n))$ for the second excitation and 0 for the first excitation, where (u_i, v_i) describe the directions of the ith RFIs. These two sets of beams enable one to directly obtain α_1 and α_2 using (9), a system of $2M$ equations with $2M$ unknowns. We name this approach, double-beam subtraction (DBS), as two sets of beams have been generated to eliminate interferers. In general, the two polarizations just need to be independent (not necessarily orthogonal), and the patterns can be accurately represented in the polarimetric sense [26]. The exploitation of polarization diversity allows one to effectively use the subtraction technique for interference suppression. For example, the weighting matrices w_1 and w_2 can be predefined so as to protect the main array beam pattern, e.g., through amplitude tapering or by creating a null in the subtracted patterns in the direction of the desired main beam [8].

A more general solution for arrays made of arbitrary antennas can be derived by rewriting (9) as

$$\begin{bmatrix} E^p(\Omega^{rfi}) \\ E^q(\Omega^{rfi}) \end{bmatrix} [w_0] = \begin{bmatrix} E^p(\Omega^{rfi}) \\ E^q(\Omega^{rfi}) \end{bmatrix} [w_p] \tag{10}$$

with vector $w_p = w_1\alpha_1 + w_2\alpha_2$. Equation (10), although being trivial, does include the subarray solution as w_p is a combination of any possible (w_1, w_2). It is worth noting that $E^p(\Omega^{rfi})$ and $E^q(\Omega^{rfi})$ are matrices of size $M \times N$, while w_p is an $N \times 1$ vector. Since $2M \ll N$, (10) is an underdetermined system of linear equations (i.e., $2M$ equations and N unknowns), for which there exists an infinity of exact solutions. In this case, the least-norm solution obtained with the Moore–Penrose pseudoinverse [23] is chosen, which will limit the loss of sensitivity, as explained in Section II-C. Therefore, we name the approach as the pseudoinverse beam subtraction (PBS) technique. One can also consider imposing zero-radiation conditions of the subtracted patterns to protect the main beam, by simply adding

$$\begin{bmatrix} E^p(\theta_0, \phi_0) \\ E^q(\theta_0, \phi_0) \end{bmatrix} [w_p] = \begin{bmatrix} 0 \\ 0 \end{bmatrix} \tag{11}$$

to (10), and solving for w_p.

C. Beam Construction Technique

Another approach to impose zero radiation in RFI directions is proposed in [27] as part of the master's thesis of one of the authors. The method was tested with identical element patterns, although the extension to include mutual coupling is straightforward and is presented here. The idea is to determine a steering vector that forms a beam in the desired direction while zeroing the radiation pattern in all the interferers' directions at the same time. Mathematically, the equations for finding the weighting vector are written as follows:

$$\begin{bmatrix} E^{co}(\Omega_0) \\ E^{co}(\Omega^{rfi}) \\ E^{X}(\Omega^{rfi}) \end{bmatrix} [w_c] = \begin{bmatrix} 1 \\ 0 \\ 0 \end{bmatrix} \tag{12}$$

where superscripts ^{co} and ^{X} denote the copolarization and cross-polarization patterns. Here, a normalized pattern is targeted. The first equation implies that the main beam points in the direction (Ω_0), which is imposed only for the copolarization pattern. This approximation is acceptable in most of the cases as, in the main beam, the copolarization pattern of the array is often several orders of magnitude greater than the cross-polarization pattern. At the same time, the rest of (12) ensures zero patterns in the RFI directions. Again, (12) is an underdetermined system of equations, with $(2M+1)$ equations and N unknowns, where an exact solution is selected using the Moore–Penrose pseudoinverse. We name the method as the pseudoinverse beam construction (PBC), since this technique forms a beam that directly includes nulls in the pattern.

To apply the PBC approach, all EEPs are first normalized, i.e., multiplied by a constant, such that the sum of the product of EEPs with the initial weight vector w_0 gives 1 in the direction of the main beam. This step simplifies the implementation of PBC and ensures the level of the main beam in the pointing direction via the first equation of (12).

PBC and PBS approaches, in (10) and (12), respectively, are found to be similar when substituting w_c by $w_0 - w_p$. However, as (12) does not explicitly use w_0 as a weighting vector for the main beam, the solutions are not the same in the two cases. Especially, when w_0 is amplitude tapered, the main beam obtained using PBC (12) can be different. In general, the solution of PBC (12) can only guarantee a correct main beam pointing direction and null pattern at RFIs. In Section III, the performance of this PBC approach will be evaluated along with the other two proposed techniques.

To evaluate the effectiveness of these approaches for the receiving arrays, the sensitivity loss is considered. We assume that signals are correlated, while noise sources are uncorrelated. The following formula is taken to measure the loss of sensitivity (this factor is proportional to G/T, the gain over noise temperature ratio) [24], [25]:

$$L = \frac{\left|\sum_{n=1}^{N} w'_n\right|^2}{N\sum_{n=1}^{N} |w_n|^2} \tag{13}$$

where $w'_n = w_n \exp(-jk(u_0 x + v_0 y))$ is the simplified model for the contribution of antenna n to the output of the beamformer, for a unit signal incident from the direction of the scan (u_0, v_0). L is maximized (equal to 1) when the array is uniformly excited. Assuming the availability of detailed noise characterization of the amplifiers, noise coupling between the antennas could be included [28]. Our numerical tests indicated that noise coupling does not fundamentally modify the need for nearly constant weight magnitudes, so that (13) remains a highly relevant and sufficiently simple criterion. It is interesting to notice that the Moore–Penrose pseudoinverse solutions of PBS (10) and PBC (12) minimize $\|w\|_2 = \|w'\|_2$, which consequently maximizes the sensitivity of the array (13). Indeed, the denominator of (13) is minimized, while the numerator approximately corresponds to the signal in the main beam, which is kept constant. Indeed, as long as nulling is not carried out too close to the main beam, the numerator of (13) is essentially unaffected during the nulling process.

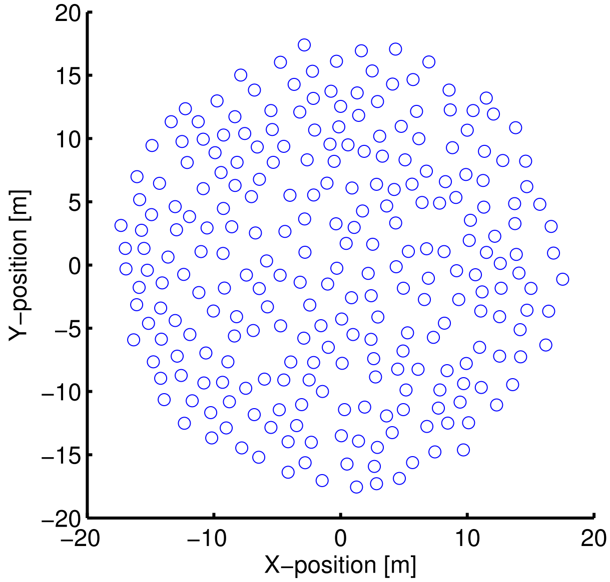

Fig. 2. Position of 256 SKALA antennas in the SKA1-LOW station, randomly distributed on a circle of 35 m in diameter with a minimum distance of 1.35 m.

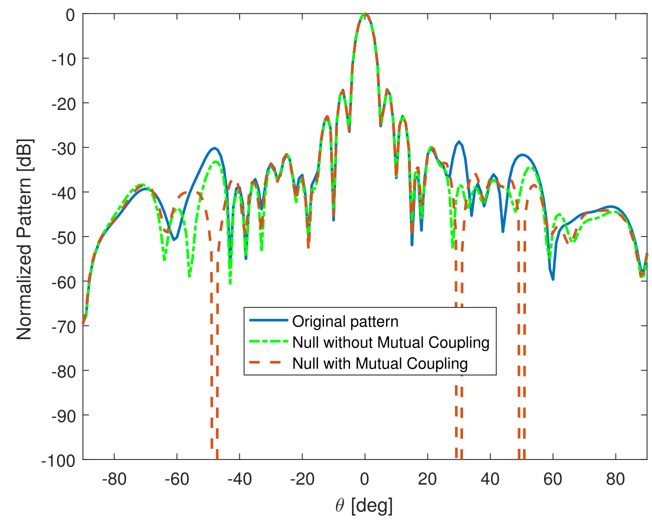

Fig. 3. Normalized copolarization pattern in $\phi = 90°$ cut of the SKA1-LOW station at 110 MHz: original pattern (solid line) obtained using w_0, null pattern without mutual coupling (dashed–dotted line), and null pattern with mutual coupling (dashed line). Three interferences at ($\phi = 90°$; $\theta = -48°, 30°, 50°$) are considered.

III. Numerical Results

In this section, the performance of all proposed techniques for interference nulling is numerically studied. First, the subtraction technique is tested for the case of pure single polarization, i.e., without cross polarization, to show the impact of mutual coupling in the null pattern. Then, the solutions from DBS (9), PBS (10), and PBC (12) approaches are applied to arrays with single- and double-polarization radiators, considering different interference scenarios. The performance will be evaluated in terms of the levels of nulls, the shape of the main beam, as well as the sensitivity loss. To pose a realistic situation, the SKA1-LOW station is considered [20]. The station is made of 256 SKALA antennas (SKALA) [20], randomly distributed over a circle of 35 m in diameter (see Fig. 2), and is currently underconstruction in Australia as part of the SKA low-frequency project. To form the array pattern, the advanced simulation technique named HARP [15], [29] is exploited to simulate the station and calculate all the EEPs. Interested readers are referred to [29] for a detailed description of HARP and its validated performance. In the following examples, the station is simulated at 110 MHz, and the array pattern calculation is accelerated as presented in [29] using the N-FFT [30]. 110 MHz is a relatively representative frequency for the SKALA antennas: on a log scale, the average operational frequency is 132 MHz, while a somewhat lower value better emphasizes the effects of (stronger) mutual coupling. To simulate the SKA1-LOW station and obtain all EEPs, HARP needs less than a minute on a desktop computer. Reference [29] describes the detailed performance of HARP and provides many validation examples.

A. Case 1: Pure Single-Polarization Arrays

The first example concerns the SKA1-LOW station with only the first excitation set active (for the first polarization), and the interferers are in the same polarization as the copolarization. Thus, the nulling needs to be performed only on the copolarization pattern. This is a simplified scenario as, in general, the polarization of the interferers can be arbitrary. The assumption, however, enables the implementation of the subtraction technique presented in Section II-A. The steering vectors w_0 and w^{rfi} are obtained by the simple delay-and-sum technique [24] to scan the beam in the desired direction and interferences, respectively. The scaling vector α is determined using (6) in two ways: 1) with the assumption that all element patterns are identical, i.e., using the isolated pattern, and thus, α is derived via an array factor and 2) using the EEPs, i.e., here only the copolarization patterns, to account for mutual coupling.

Fig. 3 shows the array patterns of the SKA1-LOW station and the null patterns in the YZ plane ($\phi = 90°$). Three interferers are assumed to be in the same plane at ($\phi = 90°$; $\theta = -48°, 30°, 50°$), i.e., coinciding with three high sidelobes. It is clear that the coefficients α obtained without mutual coupling could not suppress these sidelobes, while the one taking into account mutual coupling via EEPs effectively zeros the pattern in these directions.

B. Case 2: Arbitrary Polarization of Interferers

The second example considers a general case, where the directions of interferers are known, but the polarization can be random. As previously mentioned, a practical way to reject the RFI signals is to zero the array pattern in all these RFI directions, i.e., the constraints are forced on both copolarization and cross-polarization patterns; therefore, no interference signal appears at the output of the beamformer. The methods proposed in Sections II-B and II-C are now applied to this problem. It is noted that in the following examples, for the DBS (9) approach, both available excitations of the

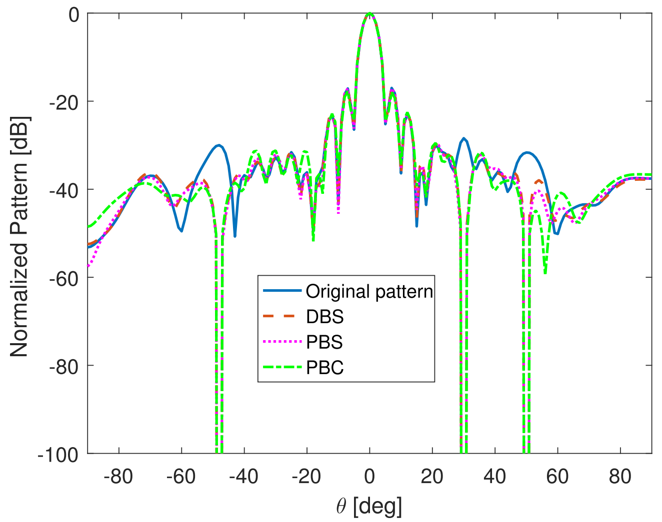

Fig. 4. Normalized array pattern in $\phi = 90°$ cut of the SKA1-LOW station at 110 MHz. Null patterns are obtained using different approaches: DBS (9), PBS (10), and PBC (12), proposed in (9), (10), and (12), respectively.

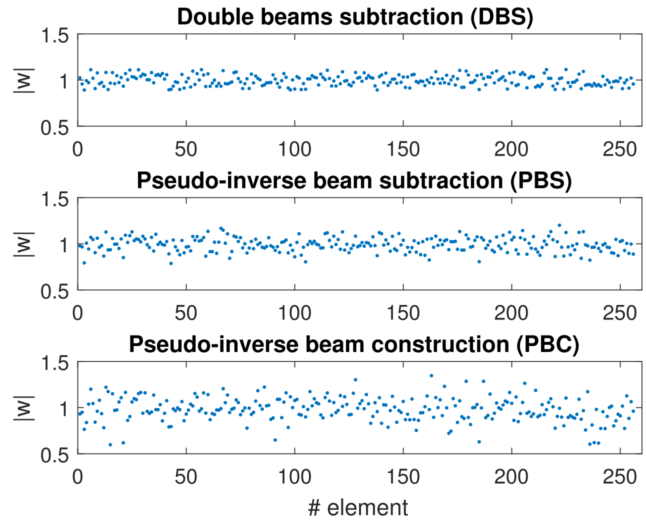

Fig. 5. Magnitude of steering vectors applied to each element of the SKA1-LOW station obtained by three approaches: DBS (9), PBS (10), and PBC (12).

TABLE I
L-FACTOR OF THE ARRAY WITH INTERFERENCE SUPPRESSION. SENSITIVITY LOSS (IN dB) ARE IN BRACKETS

Approaches	3-nulls (III-B)	36-nulls (III-D)	60-nulls (III-F)
DBS-(9)	0.995 (0.02)	0.968 (0.14)	0.903 (0.445)
PBS-(10)	0.989 (0.045)	0.89 (0.505)	0.81 (0.91)
PBC-(12)	0.963 (0.164)	0.872 (0.594)	0.792 (1.01)

SKALA antenna are exploited, and the desired beam is generated by the first excitation (first polarization), i.e., w_0 equals $\exp(-jk(u_0x + v_0y))$ for the first excitation and 0 for the second excitation, where $(u_0, v_0) = (\sin\theta_0 \cos\phi_0, \sin\theta_0 \sin\phi_0)$. The weights (w_1, w_2) in (9) are selected, as discussed in Section II-B, to generate the subtracted beams in the direction of RFIs. For the PBS (10), and PBC (12) approaches, only the first excitation is exploited.

The directions of the interference sources are the same as in Section III-A. The results for the three proposed techniques are shown in Fig. 4. The patterns now effectively exhibit zeros in all RFI directions, which confirms the performance of these alternatives. It is also noted that the array pattern is not significantly altered in the main beam and up to the second sidelobes using these proposed techniques while considering mutual coupling. This is of interest for applications such as the SKA, where accurate information about the main beam is precious for beam modeling or calibration [31].

The steering vectors obtained using these three approaches are evaluated in regard to the sensitivity factor L defined in (13), and the results are reported in the first column of Table I. DBS (9) provides the best solution, as there is only 0.02 dB loss in sensitivity thanks to the additional degrees of freedom provided by the second excitation. PBS (10) offers good results, while PBC (12) has the lowest performance. The results are still good, but the loss in sensitivity is increased from 0.02 to 0.2 dB. To better interpret the data, the obtained weights using these approaches are plotted in Fig. 5.

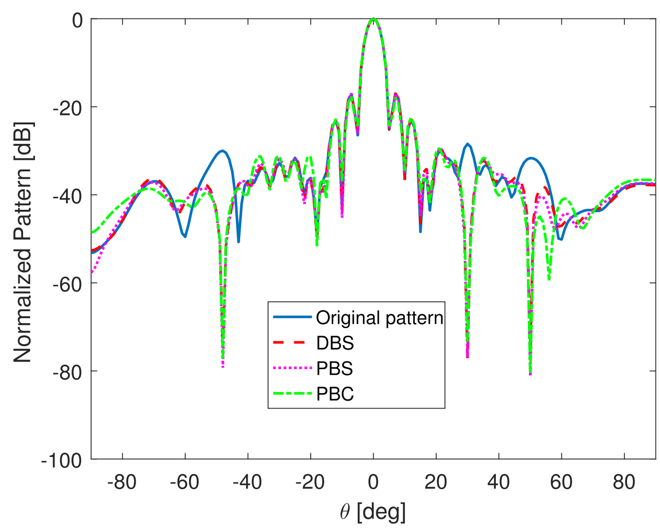

Fig. 6. Normalized array pattern in $\phi = 90°$ cut of the SKA station at 110 MHz. Similar to Fig. 4 with 1% of uncertainty added to the weighting vectors.

The weighting vector w calculated using the PBC (12) approach has the largest variation, while using the DBS (9) approach leads to the smallest variation, which is reflected by the calculated sensitivity loss L. These results confirm the advantage of properly exploiting the polarization diversity of the array in interference-nulling problems.

The robustness of the obtained solutions is now examined by adding noise to the weighting vectors. We first introduce a random 1% perturbation to the calculated weighting vectors w and recalculate the array patterns. Fig. 6 shows the radiation patterns using w with noise. Apparently, the nulls have been affected by the variation of weighting vectors. The rejection, however, is still effective as the level of the dips in the RFI directions is still near -80 dB. Adding a quite extreme 10% of uncertainty to the weights w will raise the dip levels to -60 dB, which is still acceptable in most applications. From the perspective of the stability of the

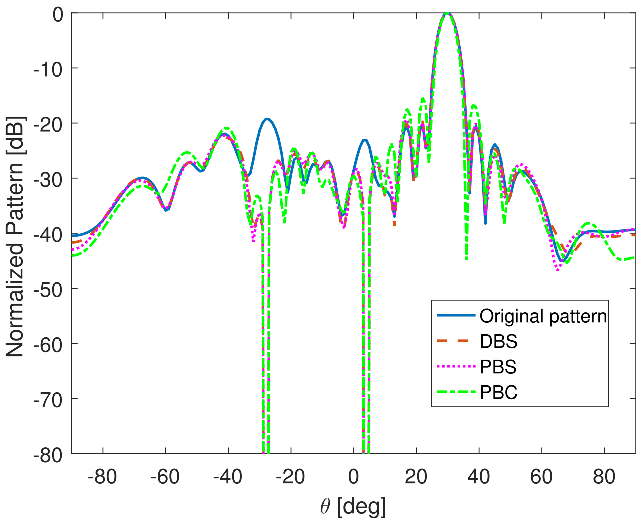

Fig. 7. Normalized array pattern in $\phi = 0°$ cut of the SKA station scanned at $(\theta, \phi) = (30°, 0°)$ at 110 MHz with amplitude tapered. The inteferers are in $(\theta, \phi) = (4°, 0°)$ and $(28°, 0°)$ directions. Null patterns are obtained using different approaches: DBS (9), PBS (10), and PBC (12), proposed in (9), (10), and (12), respectively.

solutions, the three proposed techniques perform similarly for the deterministic interference nulling.

C. Case 3: Scanned and Tapered Array

The proposed techniques are now validated with the scanned array with amplitude tapering at the same time. The amplitude of the initial excitation for element n is calculated as $w_0(n) = 1 - (r_n/r_{\max})^2/2$, with r_n the distance from the antenna n to the array's center and $r_{\max}$ the radius of a circle circumscribing the array, which is 17.5 m for the considered SKA1-LOW array shown in Fig. 2. Other tapering densities can be applied as well. The tapering selected here is an example, which is simple, while giving a sidelobe level below -20 dB (see Fig. 7) with limited sensitivity loss (about -0.17 dB). The array is phased to scan at $(\theta, \phi) = (30°, 0°)$ direction. The proposed nulling techniques are applied to suppress two interferers arriving at two peak sidelobes, located in the directions $(\theta, \phi) = (4°, 0°)$ and $(28°, 0°)$. Fig. 7 shows that these two RFIs are effectively suppressed, while the main beam is properly scanned. While the sidelobes obtained using DBS and PBS approaches marginally change with respect to the original pattern, the PBC approach produces quite high first and second sidelobes, with an increase of about 5 dB in the first sidelobe. As we already mentioned in Section II-C, the weight vector using the PBC is not constructed based on the knowledge of w_0, and thus, the sidelobe and the shape of the main beam can be different from those of the original array. The PBC, however, still effectively suppresses the RFIs and steers the beam. The DBS and PBS approaches allow maintaining the low sidelobe level achieved through tapering.

D. Case 4: 36 Randomly Located Interferers

Another example involving a large number of interferers is considered here, where 36 RFIs are randomly distributed in the sidelobe region. The results are shown in Fig. 8, and the calculated sensitivity loss is detailed in Table I. All three approaches effectively zero all the RFI sources, while the main beams and first few sidelobes are well preserved. The example confirms that these techniques are able to null simultaneously multiple interferences.

E. Case 5: Interferers Near the Main Beam

As stated in the beginning, the approaches developed in this paper are applied to reject the RFI in the sidelobe region. Interference within the main beam can be dealt with using other techniques [21]. The RFI sources, however, can be close to the main beam, i.e., in the first or second sidelobe. This section analyzes how the proposed techniques perform in this case and what are their effects on the main beam. A scenario consisting of two interferers in the $\phi = 90°$ plane at $(\theta = -12°, 7°)$ coinciding with the second and first sidelobes, respectively, is considered in this example. The three proposed approaches are applied to suppress these RFIs.

Fig. 9 shows the radiation patterns in the $\phi = 90°$ plane of the array before and after nulling. Two interferers are effectively rejected using the DBS (9), PBS (10), and PBC (12) approaches. A closer look at the main beam shows that on the left side of the pattern, $\theta = -12°$, the interferer is in the second sidelobe and the main beam is essentially preserved after nulling. However, for the right side of the pattern, $\theta = 7°$, the interferer is in the first sidelobe, and the subtracted beam is present in the initial main beam; therefore, the main beam is slightly affected by all three methods. A possible solution to preserve the whole main beam in this case is to generate a cosecant square (csc^2) pattern [32], [33] for the subtracted beam via w^{rfi} weights instead of a pencil or focused beam pattern. The falling side of the csc^2 beam is placed in the main beam of the array, such that the subtraction effect on the array beam is minimized. This solution is applicable for the DBS (9) technique as, for DBS (9), the subtracted beam can be defined in advance. As for PBS (10) and PBC (12), the weighting vectors are determined using the pseudoinverse approach, and thus, further constraints need to be imposed to protect the main beam. Techniques exploiting PBS (10) and/or PBC (12) while preserving the main beam are an open subject for future study.

F. Case 6: Regional Nulling

The extension of the previous examples consists in suppressing the signal over a specific continuous region. This is done here by zeroing the pattern in a sequence of angles spanning the region. The needed number of discrete angles is certainly depending on the size of the array through the resolution of the pattern. It is found that it is not necessary to null all these angles, as the suppression of a given interference will lower the signal level of neighboring directions as well. Thus, the number of actual nulling directions can be selected sparsely within the region. As a rule of thumb, for a 2-D array without significant eccentricity, the number of nulls needs to be of order $C(D/\lambda)^2\Omega$, where D is the diameter of the array, Ω is the solid angle of the zone to be nulled, and C is a

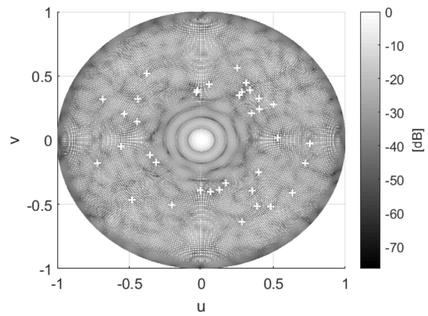

(a)

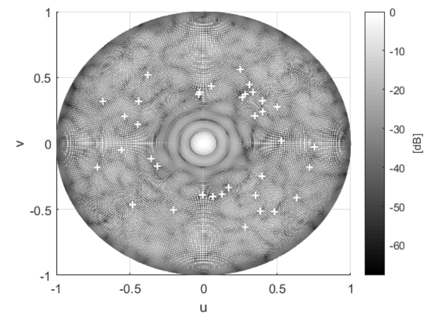

(b)

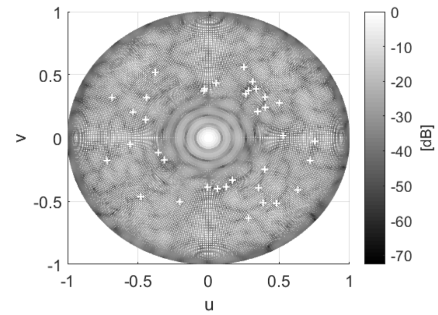

(c)

Fig. 8. Radiation pattern of the SKA1-LOW station at 110 MHz with 36 random interferences obtained using 3 proposed approaches. The nulls are marked by white cross, and their levels are below -300 dB. (a) Using DBS (9). (b) Using PBS (10). (c) Using PBC (12).

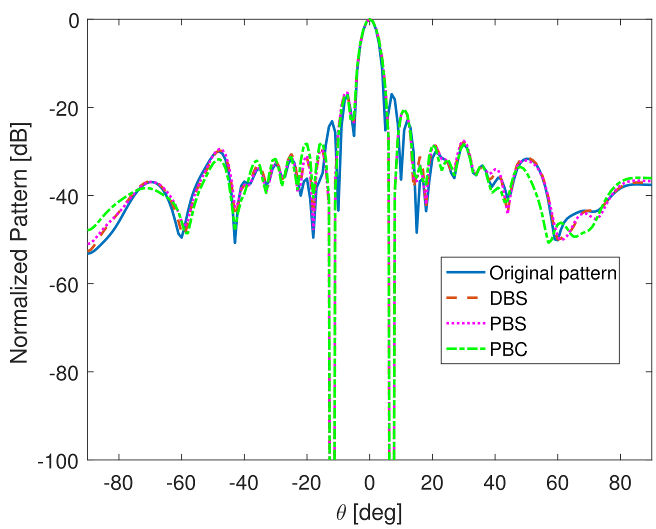

Fig. 9. Normalized array pattern in $\phi = 90°$ cut of the SKA1-LOW station at 110 MHz. Two interferences at $(\theta = -12°, 7°)$ in the "quite zone" are considered using different approaches: DBS (9), PBS (10), and PBC (12), proposed in (9), (10), and (12), respectively.

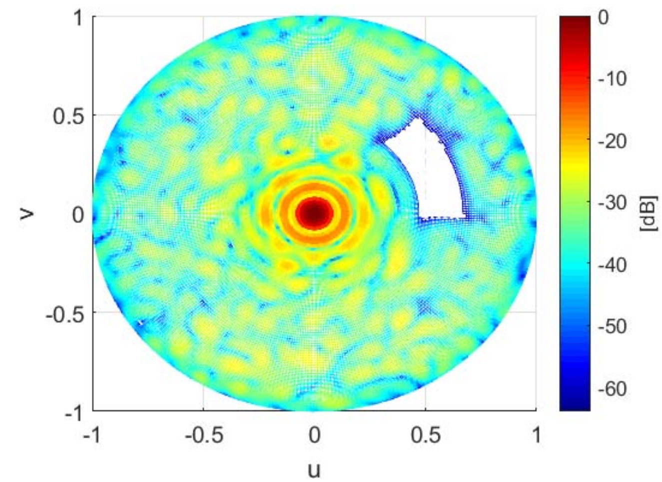

Fig. 10. Radiation pattern of the SKA1-LOW station at 110 MHz after applying weights obtained using DBS (9) for regional nulling: a wide-angle nulling with θ in [30° 40°]; ϕ in [0° 45°]: 60 nulls. All directions with levels lower than -65 dB are zeroed (white area).

constant that increases with the depth of the nulls (e.g., $C = 5$ for null levels of -60 dB). This will often avoid the situation where twice the number of nulls is greater than the number of antennas, i.e., $N \leq 2M$, and the RFIs are not effectively suppressed.

In the final example, the interferer is assumed to cover a solid angle of (θ in [30° 40°]; ϕ in [0° 45°]). The scenario resembles the interference from an extended source, such as the sun in the LOFAR or SKA systems. The proposed approaches are applied to suppress the RFIs at every $\phi = 5°$ and $\theta = 2°$, which results in 60 directions. Fig. 10 shows the radiation pattern of the SKA1-LOW station after applying weights obtained using DBS (9). Even when only 60 nulls are enforced, the suppression is effective for the predefined region with the highest level of radiation in the region below -70 dB with respect to the main beam. A similar performance has been obtained using PBS (10) or PBC (12), which is not shown here. The L factor in (13) for the weighting vectors obtained using these approaches is reported in Table I.

IV. Discussion and Perspectives

In this paper, the deterministic nulling problem has been addressed. It was shown that mutual coupling needs to be taken into account in order to properly suppress the interferers. This is done in this paper via the use of EEPs obtained using a fast full-wave simulation technique. For realistic antennas, three different approaches were proposed to effectively generate null patterns on both copolarization and cross polarization:

1) the DBS (9);
2) the PBS (10);
3) the PBC (12).

These techniques have been tested and have shown an excellent performance for the case study of the SKA1-LOW telescope station.

In particular, PBS and PBC provide quite similar performance (PBS has about 0.1 dB higher sensitivity than PBC in all tested cases). As discussed earlier, PBC might not be able to preserve the main beam pattern or the sidelobes of the original pattern [27], especially when the original pattern produced using w_0 is amplitude-tapered. PBC has its own advantages, such as correctly pointing the main beam and properly suppressing a large number of interferers, as shown in [27]. The PBC method, therefore, can be used in applications when one just needs to suppress the RFI with less emphasis on the shape of the main lobe, such as in the upcoming massive-MIMO technology or modern radar systems. While PBS is a more general method, it is applicable for any array with single or multiple polarizations.

The DBS method is the most efficient and flexible one, providing the best solution in terms of sensitivity, assuming that the array possesses two independent polarizations, which is popular nowadays. DBS effectively exploits the polarization diversity to offer several benefits such as a better control of the array beam, as was the case for the subtraction technique when applied to the array factor [8]. Both PBS and DBS can be of interest for applications such as SKA or LOFAR, where the accurate main beams need to be protected. It is worth noting that in all these examples, the coefficients and weighting vectors are efficiently obtained through direct solutions of linear systems of equations that scale with the number of elements. In addition, mutual coupling is taken into account using the EEPs, which allows accurately enforcing the zero pattern in both copolarization and cross polarization.

A topic for future study would be the integration of different synthesis techniques in the PBS, DBS, or PBC approach to better preserve the main beam. One can also consider the subarray approach to generate independent beams pointing to the interferers for the single-polarization case in (9), i.e., using a subarray to form a beam at the RFI directions. In this way, the DBS could be directly applied to the single-polarization case. The authors' first efforts showed that the subarray approach with DBS is applicable to this problem. However, the weighting vector is quite different in different subarrays, leading to a high loss of sensitivity, meaning that the variance of weights is not minimized. An optimal selection of the subarrays appears as a subject for further research.

Acknowledgment

The authors would like to thank P. Alexander and the SKA Office for the useful discussions. They would like to thank their SKA Aperture Array Design Consortium colleagues for their help and discussions on the topic. They would also like to thank the reviewers for their useful comments and suggestions.

References

[1] E. G. Larsson, O. Edfors, F. Tufvesson, and T. L. Marzetta, "Massive MIMO for next generation wireless systems," *IEEE Commun. Mag.*, vol. 52, no. 2, pp. 186–195, Feb. 2014.

[2] D. Vollbracht, "System specification for dual polarized low power X-band weather radars using phased array technology," in *Proc. Int. Radar Conf.*, Lille, France, Oct. 2014, pp. 1–6.

[3] J. D. Bregman, "Concept design for a low-frequency array," *Proc. SPIE*, vol. 4015, pp. 19–33, Jul. 2000.

[4] *The Square Kilometer Array*. Accessed: Dec. 9, 2017. [Online]. Available: https://www.skatelescope.org/

[5] S. U. Pillai, *Array Signal Processing*. New York, NY, USA: Springer-Verlag, 1989.

[6] B. D. van Veen and K. M. Buckley, "Beamforming: A versatile approach to spatial filtering," *IEEE ASSP Mag.*, vol. 5, no. 2, pp. 4–24, Apr. 1988.

[7] S. W. Ellingson and G. A. Hampson, "A subspace-tracking approach to interference nulling for phased array-based radio telescopes," *IEEE Trans. Antennas Propag.*, vol. 50, no. 1, pp. 25–30, Jan. 2002.

[8] S. W. Ellingson and W. Cazemier, "Efficient multibeam synthesis with interference nulling for large arrays," *IEEE Trans. Antennas Propag.*, vol. 51, no. 3, pp. 503–511, Mar. 2003.

[9] S. W. Ellingson, "Beamforming and interference canceling with very large wideband arrays," *IEEE Trans. Antennas Propag.*, vol. 51, no. 6, pp. 1338–1346, Jun. 2003.

[10] X. Ma, L. Lu, W. Sheng, Y. Han, and R. Zhang, "Adaptive interference nulling with pattern maintaining under mainlobe subspace and quadratic constraints," *IET Microw., Antennas Propag.*, vol. 12, no. 1, pp. 40–48, 2018.

[11] M. M. Khodier and C. G. Christodoulou, "Linear array geometry synthesis with minimum sidelobe level and null control using particle swarm optimization," *IEEE Trans. Antennas Propag.*, vol. 53, no. 8, pp. 2674–2679, Aug. 2005.

[12] T. van Luyen and T. V. B. Giang, "Interference suppression of ULA antennas by phase-only control using bat algorithm," *IEEE Antennas Wireless Propag. Lett.*, vol. 16, pp. 3038–3042, 2017.

[13] B. Fuchs, "Synthesis of sparse arrays with focused or shaped beam-pattern via sequential convex optimizations," *IEEE Trans. Antennas Propag.*, vol. 60, no. 7, pp. 3499–3503, Jul. 2012.

[14] D. González-Ovejero, E. de Lera Acedo, N. Razavi-Ghods, C. Craeye, and L. E. G. Munoz, "Non-periodic arrays for radio-astronomy applications," in *Proc. IEEE Antennas Propag. Symp.*, Spokane, WA, USA, Jul. 2011, pp. 1762–1765.

[15] Q. Queuning, C. Raucy, C. Craeye, E. Colin-Beltran, and E. de Lera Acedo, "Mutual coupling analysis in non-regular arrays of SKALA antennas with the HARP approach," in *Proc. IEEE Antennas Propag. Symp.*, Vancouver, BC, Canada, Jul. 2015, pp. 1528–1529.

[16] C. Bencivenni, M. V. Ivashina, R. Maaskant, and J. Wettergren, "Design of maximally sparse antenna arrays in the presence of mutual coupling," *IEEE Antennas Wireless Propag. Lett.*, vol. 14, pp. 159–162, 2015.

[17] H. van Bui, S. N. Jha, and C. Craeye, "Fast full-wave synthesis of printed antenna arrays including mutual coupling," *IEEE Trans. Antennas Propag.*, vol. 64, no. 12, pp. 5163–5171, Dec. 2016.

[18] J. I. Echeveste, M. Á. G. de Aza, J. Rubio, and C. Craeye, "Gradient-based aperiodic array synthesis of real arrays with uniform amplitude excitation including mutual coupling," *IEEE Trans. Antennas Propag.*, vol. 65, no. 2, pp. 541–551, Feb. 2017.

[19] H. Frid and B. L. G. Jonsson, "Compensation of radome effects in small airborne monopulse arrays by convex optimization," in *Proc. 12th Eur. Conf. Antennas Propag.*, London, U.K., Apr. 2018, pp. 1–4.

[20] E. de Lera Acedo, N. Razavi-Ghods, N. Troop, N. Drought, and A. J. Faulkner, "SKALA, a log-periodic array antenna for the SKA-low instrument: Design, simulations, tests and system considerations," *Experim. Astron.*, vol. 39, no. 3, pp. 567–594, 2015.

[21] S. W. Ellingson, J. D. Bunton, and J. F. Bell, "Removal of the GLONASS C/A signal from OH spectral line observations using a parametric modeling technique," *Astrophys. J.*, vol. 135, pp. 87–93, Jul. 2001.

[22] A. Ludwig, "The definition of cross polarization," *IEEE Trans. Antennas Propag.*, vol. AP-21, no. 1, pp. 116–119, Jan. 1973.

[23] R. Penrose, "A generalized inverse for matrices," *Math. Proc. Cambridge Philos. Soc.*, vol. 51, pp. 406–413, Jul. 1955.

[24] D. H. Johnson and D. E. Dudgeon, *Array Signal Processing: Concepts and Techniques*. Upper Saddle River, NJ, USA: Prentice-Hall, 1993.

[25] J. Grythen, "Array gain and reduction of self-noise," Norsonic AS, Oslo, Norway, Tech. Rep., 2015.

[26] T. D. Carozzi and G. Woan, "A fundamental figure of merit for radio polarimeters," *IEEE Trans. Antennas Propag.*, vol. 59, no. 6, pp. 2058–2065, Jun. 2011.

[27] V. Hamaide, "Optimal interference nulling for large arrays of coupled antennas," M.S. thesis, Univ. Catholique Louvain, Ottignies-Louvain-la-Neuve, Belgium, Jun. 2017.

[28] C. Craeye, B. Parvais, and X. Dardenne, "MoM simulation of signal-to-noise patterns in infinite and finite receiving antenna arrays," *IEEE Trans. Antennas Propag.*, vol. 52, no. 12, pp. 3245–3256, Dec. 2004.

[29] H. Bui-Van *et al.*, "Fast and accurate simulation technique for large irregular arrays," *IEEE Trans. Antenna Propag.*, vol. 66, no. 4, pp. 1805–1817, Apr. 2018.

[30] A. Dutt and V. Rokhlin, "Fast Fourier transforms for nonequispaced data," *SIAM J. Sci. Comput.*, vol. 14, no. 6, pp. 1368–1393, 1993.

[31] H. Bui-Van, C. Craeye, and E. de Lera Acedo, "Main beam modeling for large irregular arrays: The SKA1-LOW telescope case," *Exp. Astron.*, vol. 44, pp. 239–258, Dec. 2017.
[32] R. S. Elliott and G. J. Stern, "A new technique for shaped beam synthesis of equispaced arrays," *IEEE Trans. Antennas Propag.*, vol. AP-32, no. 10, pp. 1129–1133, Oct. 1984.
[33] J. Corcoles, J. Rubio, and M. Á. Gonzalez, "Spherical-wave-based shaped-beam field synthesis for planar arrays including the mutual coupling effects," *IEEE Trans. Antenna Propag.*, vol. 59, no. 8, pp. 2872–2881, Aug. 2011.

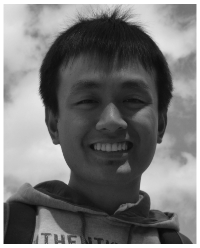

Ha Bui-Van received the Electronic and Telecommunication Engineering degree in engineering from the Hanoi University of Technology, Hanoi, Vietnam, in 2010, and the Ph.D. degree in electrical engineering from the Politecnico di Milano, Milan, Italy, in 2014.

In 2014, he was a Research Assistant with the Politecnico di Torino. From 2014 to 2018, he was with the Antenna Group, ICTEAM, Université catholique de Louvain, Louvain-la-Neuve, Belgium, as a Post-Doctoral Researcher. Since 2018, he has been with AGC Inc., Glass company, where he is involved in automotive antennas. His current research interests include the study of mutual coupling in antenna arrays, fast simulation techniques for large irregular arrays including the square kilometer arrays (SKAs) (SKA-low and SKA-mid), and array optimizations.

Valentin Hamaide received the bachelor's and master's degrees in mathematical engineering from Université catholique de Louvain, Louvain-la-Neuve, Belgium. His master's thesis was on the optimal nulling of radio interferences in the context of large arrays of coupled antennas, with an application to the square kilometer array radio telescope.

He is currently a Consultant in analytics with Deloitte Belgium, Zaventem, Belgium, where he has been involved in various data and analytics projects. His current research interests include optimization, machine learning, and the modelization of complex systems.

Christophe Craeye (M'98–SM'11) was born in Rongse, Belgium, in 1971. He received the bachelor's degree in philosophy and the master's degree in electrical engineering and the Ph.D. degree in applied sciences from the Université catholique de Louvain (UCL), Louvain-la-Neuve, Belgium, in 1994 and 1998, respectively.

From 1994 to 1999, he was a Teaching Assistant with UCL, where he carried out research on the radar signature of the sea surface perturbed by rain in collaboration with NASA and European Space Agency (ESA). From 1999 to 2001, he was a Post-Doctoral Researcher with the Eindhoven University of Technology, Eindhoven, The Netherlands, in collaboration with the Netherlands Institute for Research in Astronomy, Dwingeloo, The Netherlands, and the University of Massachusetts, Amherst, MA, USA, In 2002, he started an antenna research activity with UCL, where he is currently a Professor. He was with the Astrophysics and Detectors Group, University of Cambridge, Cambridge, U.K., in 2011. His research was funded by the Région Wallonne, European Commission, ESA, Fonds National de la recherche scientifique, and UCL. His current research interests include mutual coupling, finite antenna arrays, wideband antennas, small antennas, metamaterials, fast physical optics, and numerical methods for the fields in periodic media, with applications to communication and sensing systems.

Dr. Craeye was a recipient of the 2005–2008 Georges Vanderlinden Prize from the Belgian Royal Academy of Sciences in 2009. He was an Associate Editor of the IEEE TRANSACTIONS ON ANTENNAS AND PROPAGATION from 2004 to 2010 and the IEEE ANTENNAS AND WIRELESS PROPAGATION LETTERS from 2011 to 2017.

François Glineur received the Computer Science and Management Engineering degree and Engineering degree from Université de Mons, Mons, Belgium, and Centrale Supélec, Paris, France, in 1997, and the Ph.D. degree in applied sciences from Université de Mons in 2001.

He visited the Delft University of Technology, Delft, The Netherlands, and McMaster University, Hamilton, ON, Canada, as a Post-Doctoral Researcher. He joined the Université catholique de Louvain, Louvain-la-Neuve, Belgium, where he is currently a Professor of applied mathematics with the Engineering School and a member of the Center for Operations Research and Econometrics, Institute of Information and Communication Technologies, Electronics and Applied Mathematics. His current research interests include optimization models and methods (with a focus on convex optimization and algorithmic efficiency) and their engineering applications and nonnegative matrix factorization and applications to data analysis.

Eloy de Lera Acedo received the Ph.D. degree from the University Carlos III of Madrid, Madrid, Spain, in 2010.

He is currently a Senior Research Fellow with the Cavendish Astrophysics Group, University of Cambridge, Cambridge, U.K., where he has developed his career on instrumentation for radio astrophysics. He leads the Novel Sensors Research Group, Cavendish Astrophysics, University of Cambridge, and the Antenna and LNA Work package (AL WP) of the Aperture Array Design Consortium which is developing the array stations for the SKA telescope. Within the AL WP, he has led the design and development of SKA log-periodic antenna and its LNA. He has also lead substantial pieces of work in other international projects, such as the Hydrogen Epoch of Re-ionization Array for which he has led the design of the wideband feed within the Analog Team Group. His current research interests include ultrawideband array and antenna design, electromagnetic modeling, telescope calibration, and low-noise systems to the broader science case of 21 cm cosmology experiments.